Chem

CellPress

Article

Biodegrading plastics with a synthetic non-biodegradable enzyme

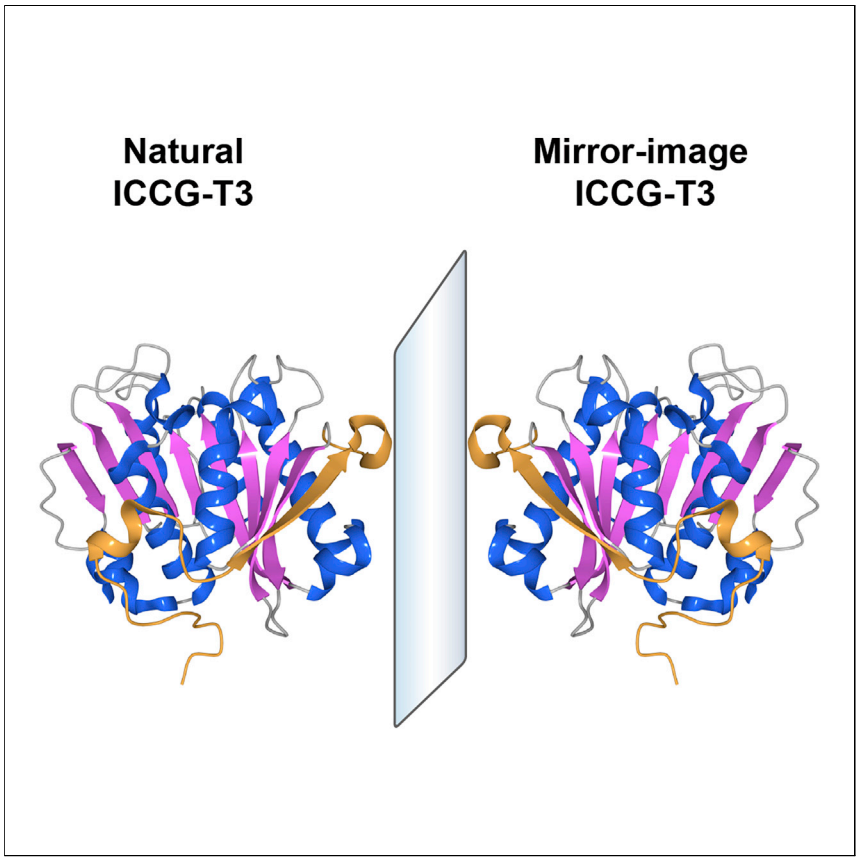

Natural enzymes capable of plastic degradation lack biostability in open environments. Jiang and colleagues chemically synthesized a non-biodegradable plastic-degrading enzyme that is composed of D-amino acids and is capable of degrading a variety of achiral plastics such as polyethylene terephthalate (PET). This work demonstrates a potential approach for gradating plastics in environments that rapidly degrade natural plastic-degrading enzymes.

Cong Guo, Li-Qun Zhang, Wenjun Jiang

jiangwj@cau.edu.cn

Highlights

Chemically synthesizing a mirror-image version of the PET hydrolase, ICCG

Degrading a variety of achiral plastics by the mirror-image PET hydrolase

Demonstrating the biostability of the mirror-image PET hydrolase

Guo et al., Chem 9, 363–376
February 9, 2023
https://doi.org/10.1016/j.chempr.2022.09.008

Chem

CellPress

Article

Biodegrading plastics with a synthetic non-biodegradable enzyme

Cong Guo,[1] Li-Qun Zhang,[1] and Wenjun Jiang[1,2,*]

SUMMARY

Biodegradation of plastics through the use of enzymes provides an attractive, environmentally friendly solution to dispose of and recycle plastic wastes. Although many natural and engineered plastic-degrading enzymes have been developed, their practical applications are hindered by their biodegradation in open environments. We reasoned that most popularly used plastics, such as polyethylene terephthalate (PET), are achiral and hence can be hydrolyzed by both the L- and D-amino acid versions of plastic-degrading enzymes. Here, we chemically synthesized a mirror-image version of the 231-aa PET hydrolase, which is capable of efficiently degrading a variety of plastics such as PET, polybutylene terephthalate (PBT), and polybutylene succinate (PBS) but meanwhile itself is resistant to biodegradation by soil extract and seawater from the environment. The synthetic mirror-image PET hydrolase demonstrates the potential of a new class of plastic-degrading, non-biodegradable mirror-image enzymes to help address the plastic pollution problem in our homochiral biosphere.

INTRODUCTION

The world-wide use of plastics has raised tremendous environmental pollution concerns. Currently, approximately 9% of plastic wastes are recycled and 12% are incinerated, with the rest of them continuing to accumulate in the natural environment.[1] Moreover, the bottom ash from incinerators has been shown to be a potential source of the microplastics (plastic particles that are less than 5 mm in size[2]), which are released into the environment.[3] Recent research shows that microplastic particles could be found in various liquid[4,5] and terrestrial environments,[6] seriously threatening marine life[7,8] and soil quality.[9,10] However, the collection of plastic wastes, especially microplastics, from the natural environment poses considerable technical and economic challenges.

Enzymatic degradation of plastics provides an ideal environmentally friendly solution.[11] In particular, polyethylene terephthalate (PET) is one of the most widely produced and used polyester plastic around the world,[12] accounting for 8% of global solid waste by weight.[13] Furthermore, the present COVID-19 pandemic outbreak has caused a several-fold increase in the use of PET polymer.[14] Several PET hydrolases have been discovered in nature[15–19] and engineered to efficiently degrade PET, with their enzymatic activity and thermostability continuously being improved upon by various methods.[12,20–23] For example, the ThermoPETase[22] and DuraPETase[23] were enhanced by ~14- and ~300-fold compared with the wild-type *Ideonella sakaiensis* PETase (*Is*PETase) at 37°C and 40°C, respectively. Moreover, ICCG (a mutant version of LCC [leaf-branch compost cutinase] with 259 aa)[12]

THE BIGGER PICTURE

Plastic pollution poses a growing global environmental problem. Enzymatic degradation of plastics presents a promising solution, and yet its susceptibility to degradation by other enzymes compromises the stability of plastic-degrading enzymes in open environments. Here, we chemically synthesized a non-biodegradable mirror-image polyethylene terephthalate (PET) hydrolase to degrade a variety of achiral plastics. The plastic-degrading, non-biodegradable mirror-image enzyme may help address the global plastic pollution problem in a variety of environments.

has been engineered to possess one of the highest enzymatic activities at ~72°C among all reported PET hydrolases.[24]

Nevertheless, biodegradation of plastic-degrading enzymes by enzymes secreted by microbes and other organisms may undermine the biostability of practical applications in open environments. We reasoned that most popularly used polyesters, such as PET, are achiral and hence can be hydrolyzed by both the L- and D-amino acid versions of the plastic-degrading enzymes (Figure 1A). Meanwhile, mirror-image enzymes themselves are resistant to biodegradation, making them potentially suitable for practical applications in open environments. So far, several mirror-image enzymes have been synthesized by combining solid-phase peptide synthesis[25] (SPPS) with native chemical ligation[26–28] (NCL), including the mirror-image HIV protease,[29] RNase,[30] DNA polymerase,[31,32] as well as RNA polymerase.[33] Here, we set out to chemically synthesize the mirror-image version of the 231-aa PET hydrolase (truncated ICCG) with D-amino acids, which efficiently degrades PET and other plastics and thus may be applied as a non-biodegradable enzyme for mitigating the plastic pollution problem in natural environments.

RESULTS

Design and synthesis of the natural and mirror-image PET hydrolase

We first compared the activity of recombinant ICCG-WT, DuraPETase, and ThermoPETase, at room temperature (~28°C). The soluble substrate ρ-nitrophenyl palmitate (ρ-NPP) binds to PET hydrolases in a similar fashion as a PET-like substrate[34] and has been used for enzymatic activity assays.[35] Degradation assays on ρ-NPP (Figure S1A) (with the product ρ-nitrophenol [ρ-NP] displaying a distinctive yellow color under alkaline conditions with an absorbance wavelength at 410 nm), suggested that the activity of DuraPETase and ThermoPETase is ~50% lower than ICCG-WT (Figure S1B). Next, we sought to evaluate the PET-degradation activity of these three proteins using PET microparticles (the crystallinities of PET microparticles is 12.3%, as shown in Figure S2A). We quantified the sum of the detected released compounds, including terephthalic acid (TPA), mono(2-hydroxyethyl)-TPA (MHET), and bis(2-hydroxyethyl)-TPA (BHET) at different time points (2, 5, and 10 days, respectively) (Figure S1C), which suggested that ICCG-WT was an optimized engineered enzyme for the total chemical synthesis.

The chemical synthesis of mirror-image ICCG-WT faced several technical challenges. In particular, the first peptide segment of ICCG-WT (ICCG-1) (Figure S3A) in our initially designed synthetic route was difficult to synthesize by SPPS directly (Figure S3B). Although we were able to synthesize ICCG-1a with isopeptide[36] at Val^{34}-Ser^{35} with reasonable yields (~3%) (Figure S3B), the subsequent NCL resulted in rather low efficiency (Figure S3C), possibly owing to the existence of a secondary structure which affected the ligation efficiency during NCL. Previous studies have shown the actual MHET-ICCG binding mode[37] and deduced 2-HE$(MHET)_3$-LCC binding mode,[12] revealing the amino acid residues in contact with the substrate (e.g., Y95, M166, H164, H242, V212, and W190), as well as the catalytic core residues (S165, H242, and D210). Based on this knowledge, we designed several N terminus-truncated versions of ICCG (-T1, -T2, -T3, and -T4) based on its structure (PDB: 6THT) to facilitate the NCL (Figures S4A and S4B; Table S1). Among them, ICCG-T2 was expressed in the inclusion body and no soluble protein could be purified from the *E. coli* strain BL21 (DE3) cells (potentially with the truncation affecting the folding and solubility of ICCG-T2), and thus only ICCG-T1, ICCG-T3, and ICCG-T4 were tested for their enzymatic activity. Degradation assays on ρ-NPP suggested that

[1]Ministry of Agriculture and Rural Affairs Key Laboratory of Pest Monitoring and Green Management, Department of Plant Pathology, College of Plant Protection, China Agricultural University, Beijing 100193, China

[2]Lead contact

*Correspondence: jiangwj@cau.edu.cn

https://doi.org/10.1016/j.chempr.2022.09.008

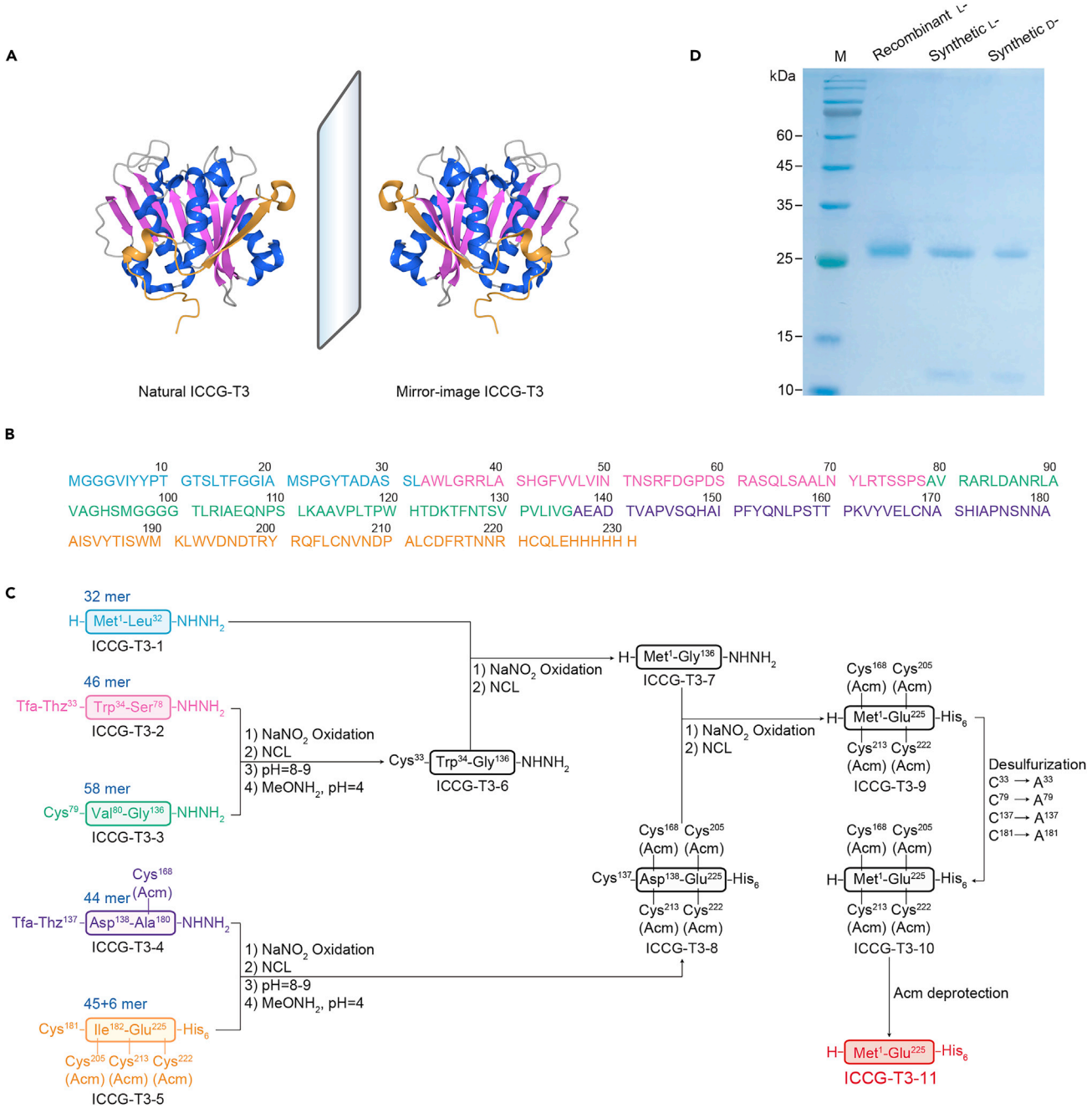

Figure 1. Synthetic natural and mirror-image ICCG-T3

(A) Structure of the PET hydrolase, ICCG (PDB: 6THT), in natural and mirror-image forms, showing the α helix in blue, β sheet in purple, and truncated sequences in yellow.

(B) Amino acid sequence of ICCG-T3, with 36 aa removed from the N terminus and a His_6 tag added to the C terminus, resulting in a total length of 231 aa, divided into five segments, the colors of which correspond to the colors used in (C).

(C) Synthetic route for synthesizing ICCG-T3.

(D) Recombinant ICCG-T3 (with a C-terminal His_6 tag) expressed and purified from *E. coli* (recombinant L-), and synthetic natural and mirror-image ICCG-T3 (synthetic L- and synthetic D-, respectively), analyzed by 12% SDS-PAGE, stained by Coomassie brilliant blue. M, protein marker.

ICCG-T1 and ICCG-T3 possessed similar enzymatic activity as wild-type ICCG at ~28°C, while the activity of ICCG-T4 was significantly compromised (Figure S4C). The specific hydrolysis activity of the four proteins on PET microparticles was determined at ~28°C, 50°C, 60°C, and 72°C, respectively (Figure S4D). We found that ICCG-T3 not only exhibited excellent activity but also thermostability, which was also assessed by differential scanning fluorimetry (DSF) (Figures S5A and S5B). In comparison, ICCG-T4 displayed impaired activity and poor thermostability, potentially due to the truncation affecting the stability of the ICCG-T4 structure. Therefore, we removed 36 aa from the N terminus according to ICCG-T3, with a His_6 tag added to the C terminus, resulting in a total size of the synthetic ICCG-T3 at 231 aa (Figures 1B and S4A).

Next, we designed a synthetic route for chemically synthesizing ICCG-T3 by assembling five peptide segments ranging in length from 32 to 58 aa (Figure 1C). We carried out the total chemical synthesis of both the natural and mirror-image versions of ICCG-T3. All the peptide segments were prepared by SPPS, purified by reversed-phase high-performance liquid chromatography (RP-HPLC), and assembled by hydrazide-based NCL with a convergent assembly strategy, followed by metal-free radical-based desulfurization[38] to convert unprotected cysteine to alanine residue after NCL. Lastly, the acetamidomethyl (Acm) groups used to protect cysteine were removed by a Pd-assisted deprotection strategy.[39] After the synthesis, ligation, purification, and lyophilization (Figures S6–S27), a total of 2 mg of the natural version of ICCG-T3 (L-ICCG-T3) was obtained, with an observed molecular mass of 25,051.4 Da (calculated molecular mass of 25,051.6 Da, Figure S16); a total of 4 mg of the mirror-image version of ICCG-T3 (D-ICCG-T3) was obtained with an observed molecular mass of 25,051.0 Da (calculated molecular mass of 25,051.6 Da, Figure S27). The synthetic L-ICCG-T3 and D-ICCG-T3 were folded by 100-fold dilution from 6 M guanidine hydrochloride (Gn·HCl) solution into the renaturation buffer.

Having synthesized and folded the synthetic L- and D-ICCG-T3, we analyzed the *in vitro* folded synthetic L- and D-ICCG-T3 by sodium dodecyl sulfate-polyacrylamide gel electrophoresis (SDS-PAGE), along with the recombinant ICCG-T3 (with a C-terminal His_6 tag) expressed and purified from *E. coli* to validate their sizes (Figure 1D). The folding of the synthetic proteins was validated by the 8-anilino-1-naphthalene sulfonate (ANS) assay[40,41] (Figure S28A) and the native PAGE (Native-PAGE) analysis (Figure S28B).

Enzymatic activity of the synthetic natural and mirror-image PET hydrolase

We next evaluated the enzymatic activity of the synthetic natural and mirror-image PET hydrolase on soluble substrate ρ-NPP. As expected, the synthetic D-ICCG-T3 hydrolyzed ρ-NPP with comparable efficiency to its natural version, including both the synthetic L-ICCG-T3 and that expressed and purified from *E. coli* (Figure S29A). Encouraged by these results, we applied L- and D-ICCG-T3 to degrade PET microparticles (ø = 10–50 μm) at ~28°C and 60°C. The specific hydrolysis activity of recombinant L- and synthetic L- and D-ICCG-T3 on PET microparticles showed no significant difference (Figure S29B). Optical microscopy images showed that the PET microparticles were gradually digested at ~28°C as time progressed (Figure 2A), with the total product release increased (Figure 2B). Most of the particles disappeared after 10 days at ~28°C (Figure 2A) and after 9 h at 60°C (Figure S29C), respectively.

Next, we applied L- and D-ICCG-T3 to degrade PET films. Scanning electron microscopy (SEM) images of the film surfaces showed that films treated with L- and

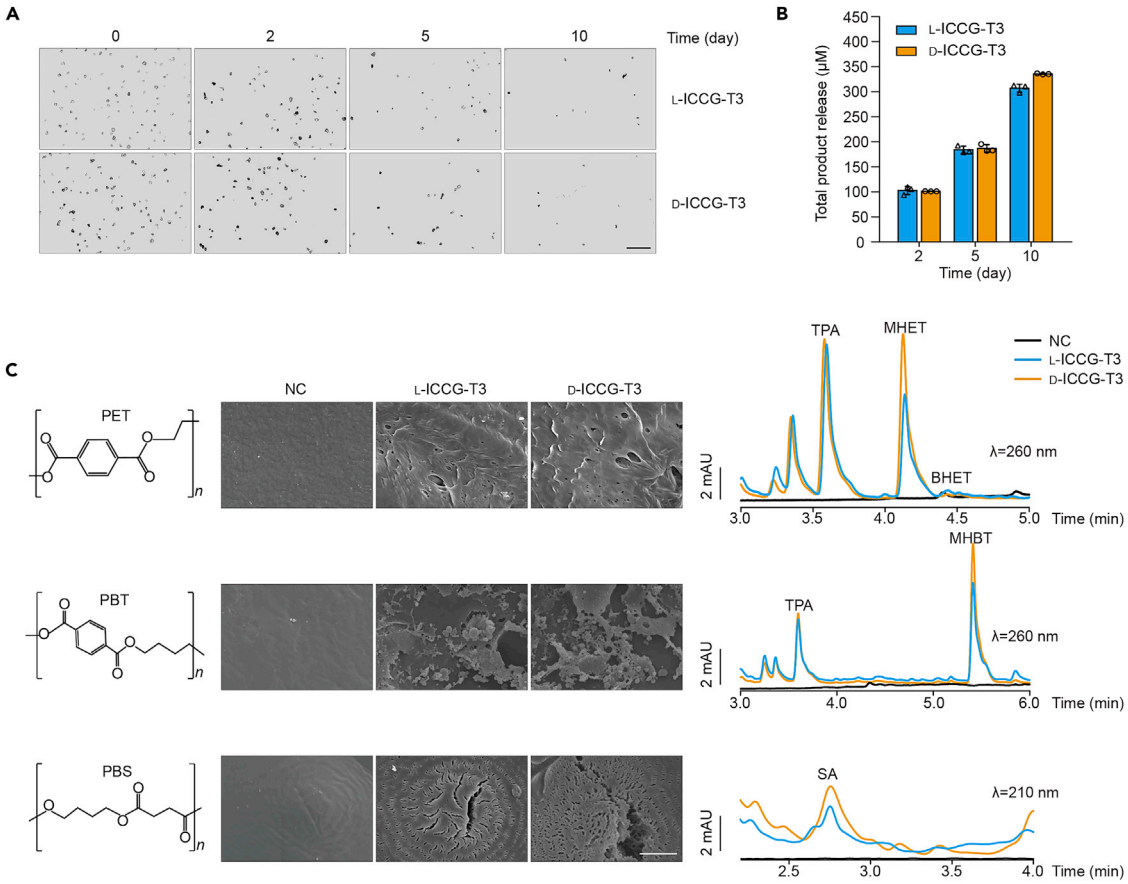

Figure 2. Enzymatic activity of the synthetic natural and mirror-image ICCG-T3

(A) Optical microscopic images of PET microparticles degraded by the synthetic L- and D-ICCG-T3, incubated in 50 mM glycine-NaOH (pH 9.0) at ~28°C for up to 10 days. Scale bars, 500 μm.

(B) Enzymatic activity of the synthetic L- and D-ICCG-T3 on PET microparticles (ø = 10–50 μm), incubated in 50 mM glycine-NaOH (pH 9.0) at ~28°C for up to 10 days, with released degradation products analyzed by HPLC and the total product release quantified as the sum of the detected released compounds, including TPA, MHET, and BHET. Error bars represent SD values obtained from triplicate experiments.

(C) Polymer structures of PET, PBT, and PBS, with SEM images and HPLC chromatograms of degradation products TPA, MHET, and BHET released from PET films, TPA and mono(4-hydroxybutyl)-TPA (MHBT) released from PBT films, and succinic acid (SA) released from PBS films, respectively, treated with the synthetic L- and D-ICCG-T3 in 50 mM glycine-NaOH (pH 9.0) at ~28°C for 15 days. NC, negative controls without the synthetic L- and D-ICCG-T3. Scale bars, 10 μm.

D-ICCG-T3 exhibited characteristic surface defects after up to 15 days, while those treated with the buffer only displayed a smooth and uniform surface (Figure 2C). In addition, we tested the degradation of both the L- and D-ICCG-T3 on polybutylene terephthalate (PBT)[23] and polybutylene succinate (PBS) (the crystallinities are 10.3% and 13.6%, respectively, as shown in Figures S2B and S2C). Our results showed that D-ICCG-T3 also possessed the abilities to degrade PBT and PBS (Figure 2C). Thus, the high enzymatic efficiency and versatility of mirror-image ICCG-T3 makes it potentially suitable for applications for degrading a wide range of achiral plastic polymers.

Stability and enzymatic activity of the synthetic natural and mirror-image PET hydrolase

To assess the stability of the mirror-image PET hydrolase, we treated both the natural and mirror-image ICCG-T3 with proteinase K, which is one of the most

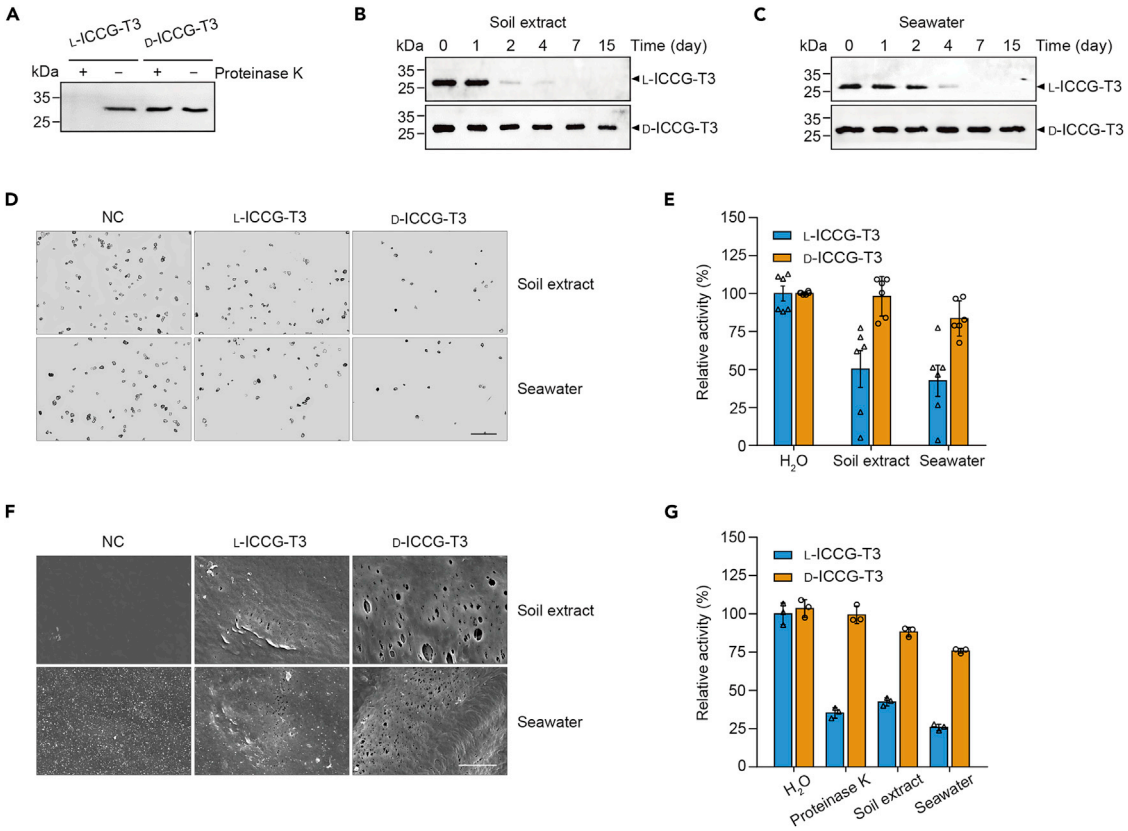

Figure 3. Stability and enzymatic activity of the synthetic natural and mirror-image ICCG-T3 in various environments

(A–C) The synthetic L- and D-ICCG-T3 digested by commercial proteinase K for 15 min, incubated with soil extract for 15 days, and seawater for 15 days at ~28°C, respectively, analyzed by His-tag blot stain.

(D) Optical microscopic images of PET microparticles after treated with synthetic L- and D-ICCG-T3 in soil extract and seawater (containing 50 mM glycine-NaOH [pH 9.0]) at ~28°C for 10 days. NC, negative controls without the synthetic L- and D-ICCG-T3. Scale bars, 500 μm.

(E) Enzymatic activity of synthetic L- and D-ICCG-T3 on PET microparticles (ø = 10–50 μm) in soil extract and seawater (containing 50 mM glycine-NaOH [pH 9.0]) at ~28 °C for 10 days, with relative activity calculated using the particle numbers and presented as percentages relative to that measured in H_2O. Error bars represent SD values obtained from six images in each experiment.

(F) SEM images of PET films after incubation with synthetic L- and D-ICCG-T3 in soil extract and seawater (containing 50 mM glycine-NaOH [pH 9.0]) at ~28°C for 15 days. NC, negative controls without the synthetic L- and D-ICCG-T3. Scale bars, 10 μm.

(G) Enzymatic activity of the synthetic L- and D-ICCG-T3 after incubating with proteinase K for 15 min, soil extract for 48 h, and seawater for 48 h, on substrate ρ-NPP in 50 mM Tris-HCl (pH 8.0) at ~28°C for 1 h, with relative activity calculated using the measured ρ-NP as percentages relative to that measured in H_2O. Error bars represent SD values obtained from triplicate experiments.

commonly used laboratory model enzymes to digest proteins. His-tag blot stain showed that the natural ICCG-T3 was rapidly digested by proteinase K, and the degradation assay with soluble substrate ρ-NPP showed that the natural ICCG-T3 had lost most of its enzymatic activity. In comparison, the mirror-image ICCG-T3 was entirely resistant to proteinase K digestion, with the enzymatic activity retained (Figures 3A, 3G, and S30A).

Moreover, we investigated the stability of the natural and mirror-image ICCG-T3 in both soil extract and seawater (microbial compositions shown in Figure S31 and Table S2) for potential applications in degrading microparticles in soil and marine environments. Samples harvested at six time points (0, 1, 2, 4, 7, and 15 days) with His-tag blot stain showed that the mirror-image ICCG-T3 persisted for more than 15 days in soil extract and seawater. In comparison, the natural ICCG-T3 was rapidly degraded within 2–4 days (Figures 3B and 3C).

To further test the enzymatic activity of natural and mirror-image ICCG-T3 in open environments, we incubated the synthetic L- and D-ICCG-T3 in soil extract and seawater for 48 h, after which soluble substrate ρ-NPP was added to test their enzymatic activity. Our results showed that the enzymatic activity of the mirror-image ICCG-T3 in soil extract and seawater was significantly higher than that of the natural ICCG-T3 (Figures 3G and S30A), despite the slightly decreased enzymatic activity of mirror-image ICCG-T3 in seawater, likely due to the high salt concentration as we further demonstrated in a control experiment (Figure S30B).

Furthermore, we incubated the natural and mirror-image ICCG-T3 with PET microparticles in soil extract and seawater for up to 10 days. As expected, the enzymatic activity of the natural ICCG-T3 in soil extract and seawater was significantly reduced compared with that treated with pure water. In comparison, the enzymatic activity of the mirror-image ICCG-T3 was largely unaffected by soil extract and seawater (Figures 3D and 3E). We also treated PET films by natural and mirror-image ICCG-T3 in soil extract and seawater for up to 15 days. SEM images displayed much more extensive degradation, both in the number and size of holes, on the PET films treated with D-ICCG-T3 than those with L-ICCG-T3 (Figure 3F). Therefore, while the natural PET hydrolase was rapidly degraded, with its enzymatic activity severely compromised in natural environment, the stability and activity of mirror-image PET hydrolase was largely unaffected.

DISCUSSION

In this work, we have reported the engineering and chemical synthesis of a mirror-image PET hydrolase with D-amino acids, capable of degrading various achiral plastic polymers such as PET, PBT, and PBS. The non-biodegradable nature of this D-protein makes it promising for broad applications in detecting and degrading plastic wastes in open environments. Thus, despite the high cost and limited availability of synthetic enzymes at the moment, our initial demonstration of a non-biodegradable plastic-degrading enzyme reported in this work suggests that its potential applications could be different from the conventional ones (e.g., being used as immobilized enzymes, recyclable and reusable for degrading uncollectable micro- and nano-plastics in soil or liquid environments) and could be potentially further expanded in future research. For example, recent studies have provided evidence of microplastics existing in human gut,[42] human placenta,[43] and human blood.[44] Thanks to the bio-orthogonal nature of the mirror-image PET hydrolase and the low immunogenicity of D-amino acid proteins,[45] they may even potentially be used as synthetic enzymatic drugs to help digest and clear microplastic particles from the human body. Such possibilities and other application scenarios can be explored further in future studies on a variety of non-biodegradable plastic-degrading enzymes.

Potential factors that may ultimately limit the practical applications of mirror-image PET hydrolase include the low synthesis yield and high costs of synthesis. However, an improved peptide synthesis method, such as automated fast-flow peptide synthesis[46] (AFPS), and optimized synthetic strategies such as split-protein design may help to address these issues.[32] In addition, the raw material costs for chemically synthesizing D-proteins are rather low for most of the 9-fluorenylmethyloxycarbonyl (Fmoc)-D-amino acids, with the exception of D-isoleucine, and hence systematic isoleucine substitution may also drastically reduce the cost of synthesizing the D-protein.[32]

Additionally, recent studies have attempted to establish stable marine bacterial communities that efficiently degrade PET wastes,[47] as the mixed floras have greater

environmental adaptability, higher degradation efficiencies, and a broader usage scope for bioremediation,[48] and yet PET can be finally catabolized into CO_2 if treated with microbes.[19] In comparison, the final products of PET treated with PETase or LCC are TPA and ethylene glycol instead,[21] and under certain conditions, TPA can also be reused after purification.[12,24] Thus, the use of non-biodegradable plastic-degrading enzymes provides an alternative, potentially economically viable and environmentally friendly solution for plastic degradation.

The synthesized mirror-image PET hydrolase presents an initial proof-of-concept for producing a new class of plastic-degrading, non-biodegradable mirror-image enzymes. Currently, we chose to synthesize the 231-aa PET hydrolase (ICCG-T3) for its small size, thermostability, and high enzymatic activity both at room and elevated temperatures. Many other natural cutinases and PETases have been shown to possess abilities to degrade PET and other achiral plastics,[24,47,49] which can also become potential targets for the total chemical synthesis of their mirror-image versions. Furthermore, recent developments in protein design[50,51] may also present new opportunities for designing and engineering non-biodegradable mirror-image enzymes that degrade chiral plastics.

EXPERIMENTAL PROCEDURES

Resource availability

Lead contact

Further information and requests for resources should be directed to and will be fulfilled by the lead contact, Wenjun Jiang (jiangwj@cau.edu.cn).

Materials availability

All materials generated in this study are available from the lead contact without restriction.

Data and code availability

This study did not generate any datasets.

Synthetic route design

The synthetic segments and routes designed mainly based on the principle of NCL in the literature,[26,28] which has proven to be an efficient ligation reaction between the polypeptide thioester and the N-terminal Cys peptide. However, the abundance of Cys in most proteins is low, whereas Cys can be converted into Ala by desulfurization.[27] With only 4 Cys in ICCG-WT and their location are unsuitable for ligation to produce full-length protein, we divided the whole protein into 5 segments by selecting the N-terminal Ala sites, and each peptide contained 32–58 amino acids, at suitable lengths for SPPS.

Fmoc-based SPPS

All peptides were efficiently synthesized by Fmoc-based SPPS on the Liberty Blue automated microwave peptide synthesizer (CEM Corporation, North Carolina, USA). ICCG-T3-(1-4) were synthesized on Fmoc-hydrazine 2-chlorotrityl chloride resin to prepare peptide hydrazides.[52] ICCG-T3-5 with a carboxy-terminal carboxylate was synthesized on Wang Chemmatrix resin (CSBio) preloaded with the first C-terminal residue. The first residue was manually attached to the Wang Chemmatrix resin by a double coupling method. In the first coupling reaction, amino acid was coupled for 1 h at 30°C using 4 equivalents (equiv) of amino acid, 3.8 equiv *O*-(6-chlorobenzotriazol-1-yl)-*N*, *N*, *N*′, *N*′-tetramethyluronium hexafluorophosphate (HCTU) and 8 equiv *N*, *N*-Diisopropylethylamine (DIEA), and the resin was

washed with *N*, *N*-dimethylformamide (DMF) and dichloromethane. Without deprotection, the second coupling reaction was carried out overnight at 25°C with 4 equiv amino acid, 4 equiv ethyl cyanoglyoxylate-2-oxime (Oxyma) and 4 equiv *N*, *N*′-diisopropylcarbodiimide (DIC). All resins were swelled in DMF for 10 min before use. The Fmoc groups of both the resin and the assembled amino acids were removed by treating with 20% piperidine and 0.1 M Oxyma in DMF at 85°C. Amino acid coupling was carried out at 85°C with 4 equiv Fmoc-amino acids, 4 equiv Oxyma, and 8 equiv DIC. The coupling reactions for Fmoc-Cys (Trt)-OH and Fmoc-His (Trt)-OH were carried out at 50°C for 10 min to avoid side reactions at high temperature. Isodipeptide building blocks Fmoc-Val34-Ser35^{iso}-OH (in segment ICCG-1a) was incorporated during SPPS.[53] Trifluoroacetyl thiazolidine-4-carboxylic acid-OH[54] was coupled using Oxyma/DIC activation at room temperature overnight. 2,4-Dimethoxybenzyl (DMB)-Gly at 57 (in ICCG-T3-2) was incorporated during SPPS to improve the purity of peptide. Fmoc-Cys (Acm)-OH was used at positions 168, 205, 213, and 222 to avoid potential complications during the desulfurization step. After the completion of peptide chain assembly, peptides were cleaved from resin using H_2O/thioanisole/triisopropylsilane/1,2-ethanedithiol/trifluoroacetic acid (TFA) (0.5/0.5/0.5/0.25/8.25). The cleavage reaction took 3 h under agitation at 25°C. After N_2 bubbling, cold Et_2O precipitation, and centrifugation, the crude peptides were obtained. The crude peptides were dissolved in CH_3CN/H_2O, analyzed by RP-HPLC and electrospray ionization mass spectrometry (ESI-MS), and purified by semi-preparative RP-HPLC.

NCL

The peptide segment with C-terminal hydrazide was dissolved in acidified ligation buffer (0.1 M phosphate, 6 M Gn·HCl, pH 3.0). The mixture was cooled in an ice-salt bath (−12°C), and 10 equiv sodium nitrite ($NaNO_2$) in acidified ligation buffer (0.5 M, pH 3.0) was added. The oxidation process was conducted in ice-salt bath under stirring for 23 min, followed by adding 40 equiv 4-Mercaptophenylacetic acid (MPAA) in ligation buffer (pH of MPAA solution was adjusted to 5.0–6.0) and 1 equiv N-terminal Cys peptide. The pH of the solution was adjusted to 6.5–6.8 at room temperature and the reaction mixture was stirred overnight. Then, 150 mM tris (2-carboxyethyl) phosphine hydrochloride (TCEP·HCl) in ligation buffer (pH of the solution was adjusted to 7.0) was added to dilute the system twice and the reaction system was kept at room temperature for 20 min with stirring. Finally, the ligation product was analyzed by HPLC and ESI-MS, and purified by semi-preparative HPLC.

Desulfurization

Cysteine-containing peptide (1.5 mg/mL) was dissolved in desulfurization buffer (0.1 M aqueous phosphate buffer containing 6 M Gn·HCl, 200 mM TCEP, 40 mM reduced L-glutathione, and 20 mM 2, 2′-azobis [2-(2-imidazolin-2-yl) propane] dihydrochloride [VA-044], pH 6.8). The mixture was stirred at 37°C overnight, and the desulfurization product was analyzed by RP-HPLC and ESI-MS, and purified by semi-preparative RP-HPLC.

Acm deprotection

The Acm group was removed by the Pd-assisted deprotection strategy. Acm-protected peptide was dissolved in Acm deprotection buffer (aqueous solution of 6 M Gn·HCl, 0.1 M phosphate, and 40 mM TCEP, pH 7.0) to a final concentration of 1 mM, after which 40 equiv palladium chloride ($PdCl_2$) was added. The reaction mixture was incubated with agitation at 30°C for 3 h. DL-1, 4-dithiothreitol (DTT) was added to 50 mM final concentration to quench the reaction. The reaction mixture was stirred for 1 h and purified by semi-preparative RP-HPLC.

RP-HPLC and ESI-MS

All RP-HPLC analyses and purifications of the peptides were carried out using Shimadzu Prominence HPLC systems with SPD-20A detectors and LC-20AT solvent delivery units. An Ultimate XB-C4 column (Welch, 300 Å, 5 μm, 4.6 × 250 mm) was used for analysis at a flow rate of 1 mL/min, to monitor the ligation reaction and analyze the purity of the peptide products. Ultimate XB-C4 column (Welch, 300 Å, 5 μm, 10 × 250 mm) and Ultimate XB-C4 column (Welch, 120 Å, 5 μm, 10 × 250 mm) were used to separate the ligation products at a flow rate of 4 mL/min. C18 column (Welch, 120 Å, 5 μm, 21.2 × 150 mm) and C4 column (Welch, 300 Å, 5 μm, 21.2 × 150 mm) were used to separate the crude peptides at a flow rate of 8 mL/min. The purified products were characterized by ESI-MS on a Shimadzu LC/MS-2020 system. HPLC analysis of the degradation assay was performed on an Agilent 1290 Infinity II system (Agilent Technologies, USA) equipped with an Eclipse Plus-C18 column (Agilent, 3.5 μm, 4.6 × 100 mm). Separation was performed at 25°C. TPA, MHET, BHET, and MHBT were separated using a gradient of acetonitrile (5%–90%) in 0.1% TFA at 260 nm with a flow rate of 1 mL/min. SA was separated using 20 mM phosphate buffer solution (pH 2.9) at 210 nm with a flow rate of 1 mL/min. Assays were performed in triplicates and evaluated accordingly.

Protein folding

Synthetic ICCG-T3 (1 mg) was dissolved in denaturing buffer (6 M Gn·HCl, 20 mM Tris-HCl, pH 8.0, 300 mM NaCl, 20 mM DTT, 50 mM NaAc, 0.5 mM ethylenediaminetetraacetic acid [EDTA], 10% glycerol) at a concentration of 1 mg/mL. The solution was diluted to 100-fold into renature buffer (20 mM Tris-HCl, pH 8.0, 300 mM NaCl, 20 mM DTT, 50 mM NaAc, 0.5 mM EDTA, 10% glycerol). The sample was placed in a 4°C shaker overnight (100 rpm), after which the solution was heated to 65°C for 30 min to precipitate thermolabile peptides, which were subsequently removed by centrifugation at 10,000 g for 30 min at 4°C. The supernatant was concentrated and dialyzed against a storage buffer (20 mM Tris-HCl, pH 8.0, 300 mM NaCl, 50% glycerol) (50% glycerol can best help to preserve the enzymatic activity at −20°C during long-term storage).

ANS assay

The folding of the synthetic proteins was validated by the ANS assay. 10 μM (final concentration) proteins in Tris-HCl buffer (20 mM Tris-HCl, pH 8.0, 300 mM NaCl) were mixed with 50 μM (final concentration) sodium 8-anilino-1-naphthalenesulfonate (ANS-Na)for 1–2 h in dark at 28°C. For fluorescence measurements, ANS was excited at 380 nm on the SpectraMax i3x (Molecular Devices, USA), and emission was measured from 405 to 620 nm.

Soil extract and seawater preparation

The seawater was taken from Haiyang, Shandong Province, China. The soil samples were taken from Tianxing Township, Qiubei County, Yunnan Province, China. 2 g soil sample was suspended in 10 mL deionized water and shaken at 30°C for 2–3 h. Filter membranes (0.45 μm) were used to remove insoluble solid impurities. To get more information about the soil extract and seawater samples, we used quantitative 16S ribosomal DNA (rDNA) PCR assay for determination of bacterial nucleic acid load before and after filtration. All bacteria in 10 mL 0.2 g/mL soil extract and 250 mL seawater unfiltered or filtered by 0.45 or 0.22 μm membrane filters were collected in a 0.22 μm filter membrane, respectively. Then using the DNeasy PowerSoil Pro Kit (QIAGEN, Germany) to extract the whole genome, amplifying the V3–V4 region and calculating the abundance of bacteria in filtered samples relative to bacteria in unfiltered samples. We amplified the V3–V4 region and calculated the relative

abundance of bacteria. The result was shown in Figure S31. Furthermore, we cultured bacteria before and after filtration respectively by using four kinds of mediums (Lysogeny Broth [LB], Trypic Soy Broth Medium [TSB], Potato Dextrose Agar [PDA], and R2A medium) at 28°C. After isolating single bacterial colonies, we amplified and sequenced the 16S rDNA fragments using 27F/1492R primers. Then the genus-level identifications were determined by the basic local alignment search tool (BLAST). The primers used were shown in Table S1 and the number and identification of isolated colonies were shown in Table S2.

Enzymatic activity assay with ρ-NPP substrate

To compare the enzymatic activity, ρ-NPP was chosen as a substrate for enzyme assay. The ρ-NP released from the substrate displays a distinctive yellow color under alkaline conditions with an absorbance wavelength at 410 nm by microplate reader SpectraMax i3x (Molecular Devices, USA). The reaction buffer contained 20 μL 500 mM Tris-HCl buffer (pH 8.0), 20 μL 8 mM ρ-NPP, 8 μL 2 μM enzymes and 152 μL ddH_2O or environmental samples (soil extract and seawater). After incubation at ~28°C for 1 h, trichloroacetic acid solution was added to stop the reaction, then Na_2CO_3 solution was added to develop color. One unit of enzymatic activity was defined as the amount of enzyme released 1 μmol of ρ-NP per minute.[55]

Enzymatic activity assay with PET microparticle substrate

To evaluate the PET-hydrolytic activity of DuraPETase, ThermoPETase, ICCG-WT, and its variants, and synthetic natural or mirror-image ICCG-T3, PET microparticles were used as the substrate for degradation assays. The PET microparticles (80 μL) were added in 420 μL reaction buffer containing 50 μL 500 mM glycine-NaOH buffer (pH 9.0) (pH 9.0 was the best condition for activity of either PETase or ICCG),[12,22,23] 20 μL 2 μM enzymes and 350 μL ddH_2O or environmental samples (soil extract and seawater). The reaction mixture was incubated at ~28°C for 10 days or at higher temperature (50°C, 60°C, and 72°C) for 9 h. Samples were harvested at multiple time points. After centrifugation at maximum speed for 15 min, the supernatant was analyzed by HPLC immediately and the precipitated microparticles were resuspended in dimethyl sulfoxide (DMSO). Then, pipetted 5 μL solution for optical microscope observation. We had taken six images per measurement for statistics. The ImageJ software (https://imagej.nih.gov/ij) was used to count the numbers.

Enzymatic activity assay with polymer film substrate

The PET, PBT, and PBS films (⌀ = 5 mm) were soaked in 200 μL buffer containing 20 μL 500 mM glycine-NaOH buffer (pH 9.0), 8 μL 2 μM synthetic natural or mirror-image ICCG-T3 and 172 μL ddH_2O or environmental samples (soil extract and seawater). The reaction mixture was incubated at ~28°C for 15 days.

Synthetic natural or mirror-image ICCG-T3 degradation with proteinase K

For protease digestion, 2.5 μg synthetic natural or mirror-image ICCG-T3 in 25 μL storage buffer was treated with 0.5 μL of thermolabile proteinase K for 15 min at ~28°C followed by inactivation for 10 min at 55°C. Then, 10 μL of mixture was taken for His-tag blot stain and 4 μL of mixture was taken for enzymatic activity assay with ρ-NPP substrate.

Synthetic natural or mirror-image ICCG-T3 degradation with soil extract and seawater

For environmental sample digestion, 10 μg synthetic natural or mirror-image ICCG-T3 in 20 μL storage buffer was incubated with 80 μL soil extract or seawater at ~28°C for up to 15 days. Then, 10 μL of mixture was taken for His-tag blot stain at six time

points (0, 1, 2, 4, 7, and 15 days). After incubation for 48 h, 4 μL of mixture was taken for enzymatic activity assay with ρ-NPP substrate.

His-tag blot stain

Protein samples were resolved by 12% SDS-PAGE and transferred onto a nitrocellulose membrane (Merck Millipore, Germany). The nitrocellulose membrane was stained with 20 mL of ready-to-use InVision His-tag In-gel Stain (ThermoFisher scientific, USA) for 20 min at room temperature. After rinsing the membrane briefly with deionized water for 2 min, an imager (Azure biosystems C600, USA) was used to visualize and image the membrane.

SEM

After cultivation, the films were washed 3 times each with 1% SDS, distilled water, and ethanol. Samples were sputter-coated with gold in an ion sputter (EIKO IB-3, Japan). The morphology of PET, PBT, and PBS with and without enzyme exposure was examined by S-3400N (Hitachi, Tokyo, Japan) SEM at an accelerating voltage of 10 kV.

SUPPLEMENTAL INFORMATION

Supplemental information can be found online at https://doi.org/10.1016/j.chempr.2022.09.008.

ACKNOWLEDGMENTS

We thank Q. Deng, C. Fan, H. Liu, Y. Xu, J. Zhang, and R. Zhao for assistance with the chemical synthesis of ICCG-T3. This work was supported in part by funding from the National Natural Science Foundation of China (grant nos. 31901845, 31572045, and 31872020).

AUTHOR CONTRIBUTIONS

C.G. performed the experiments. All authors analyzed and discussed the results. W.J. designed and supervised the study and wrote the paper with input from all authors.

DECLARATION OF INTERESTS

The authors have filed a provisional patent application related to this work.

Received: March 1, 2022
Revised: July 4, 2022
Accepted: September 13, 2022
Published: October 4, 2022

REFERENCES

1. Geyer, R., Jambeck, J.R., and Law, K.L. (2017). Production, use, and fate of all plastics ever made. Sci. Adv. *3*, e1700782.

2. Thompson, R.C., Olsen, Y., Mitchell, R.P., Davis, A., Rowland, S.J., John, A.W., McGonigle, D., and Russell, A.E. (2004). Lost at sea: where is all the plastic? Science *304*, 838.

3. Yang, Z., Lü, F., Zhang, H., Wang, W., Shao, L., Ye, J., and He, P. (2021). Is incineration the terminator of plastics and microplastics? J. Hazard. Mater. *401*, 123429.

4. Li, W.C., Tse, H.F., and Fok, L. (2016). Plastic waste in the marine environment: a review of sources, occurrence and effects. Sci. Total Environ. *566–567*, 333–349.

5. Li, J., Liu, H., and Paul Chen, J. (2018). Microplastics in freshwater systems: a review on occurrence, environmental effects, and methods for microplastics detection. Water Res. *137*, 362–374.

6. Yang, L., Zhang, Y., Kang, S., Wang, Z., and Wu, C. (2021). Microplastics in soil: a review on methods, occurrence, sources, and potential risk. Sci. Total Environ. *780*, 146546.

7. Gola, D., Tyagi, P.K., Arya, A., Chauhan, N., Agarwal, M., Singh, S.K., and Gola, S. (2021). The impact of microplastics on marine environment: a review. Environ. Nanotechnol. Monit. Manag. *16*, 100552.

8. Lu, Y., Zhang, Y., Deng, Y., Jiang, W., Zhao, Y., Geng, J., Ding, L., and Ren, H. (2016). Uptake and accumulation of polystyrene microplastics in zebrafish (Danio rerio) and toxic effects in liver. Environ. Sci. Technol. *50*, 4054–4060.

9. Khalid, N., Aqeel, M., and Noman, A. (2020). Microplastics could be a threat to plants in terrestrial systems directly or indirectly. Environ. Pollut. *267*, 115653.

10. Kumar, M., Xiong, X., He, M., Tsang, D.C.W., Gupta, J., Khan, E., Harrad, S., Hou, D., Ok, Y.S., and Bolan, N.S. (2020). Microplastics as pollutants in agricultural soils. Environ. Pollut. *265*, 114980.

11. Mohanan, N., Montazer, Z., Sharma, P.K., and Levin, D.B. (2020). Microbial and enzymatic degradation of synthetic plastics. Front. Microbiol. *11*, 580709.

12. Tournier, V., Topham, C.M., Gilles, A., David, B., Folgoas, C., Moya-Leclair, E., Kamionka, E., Desrousseaux, M.L., Texier, H., Gavalda, S., et al. (2020). An engineered PET depolymerase to break down and recycle plastic bottles. Nature *580*, 216–219.

13. George, N., and Kurian, T. (2014). Recent developments in the chemical recycling of postconsumer poly(ethylene terephthalate) waste. Ind. Eng. Chem. Res. *53*, 14185–14198.

14. IHS Markit (2021). PET Polymer: Chemical Economics Handbook (IHS Markit). https://ihsmarkit.com/products/pet-polymer-chemical-economics-handbook.html.

15. Müller, R.J., Schrader, H., Profe, J., Dresler, K., and Deckwer, W.D. (2005). Enzymatic degradation of poly(ethylene terephthalate): rapid hydrolyse using a hydrolase from *T. fusca*. Macromol. Rapid Commun. *26*, 1400–1405.

16. Ronkvist, Å.M., Xie, W., Lu, W., and Gross, R.A.J.M. (2009). Cutinase-catalyzed hydrolysis of poly(ethylene terephthalate). Macromolecules *42*, 5128–5138.

17. Ribitsch, D., Acero, E.H., Greimel, K., Eiteljoerg, I., Trotscha, E., Freddi, G., Schwab, H., and Guebitz, G.M. (2012). Characterization of a new cutinase from *Thermobifida alba* for PET-surface hydrolysis. Biocatal. Biotransform. *30*, 2–9.

18. Sulaiman, S., Yamato, S., Kanaya, E., Kim, J.J., Koga, Y., Takano, K., and Kanaya, S. (2012). Isolation of a novel cutinase homolog with polyethylene terephthalate-degrading activity from leaf-branch compost by using a metagenomic approach. Appl. Environ. Microbiol. *78*, 1556–1562.

19. Yoshida, S., Hiraga, K., Takehana, T., Taniguchi, I., Yamaji, H., Maeda, Y., Toyohara, K., Miyamoto, K., Kimura, Y., and Oda, K. (2016). A bacterium that degrades and assimilates poly(ethylene terephthalate). Science *351*, 1196–1199.

20. Then, J., Wei, R., Oeser, T., Barth, M., Belisário-Ferrari, M.R., Schmidt, J., and Zimmermann, W. (2015). Ca^{2+} and Mg^{2+} binding site engineering increases the degradation of polyethylene terephthalate films by polyester hydrolases from *Thermobifida fusca*. Biotechnol. J. *10*, 592–598.

21. Austin, H.P., Allen, M.D., Donohoe, B.S., Rorrer, N.A., Kearns, F.L., Silveira, R.L., Pollard, B.C., Dominick, G., Duman, R., El Omari, K., et al. (2018). Characterization and engineering of a plastic-degrading aromatic polyesterase. Proc. Natl. Acad. Sci. USA *115*, E4350–E4357.

22. Son, H.F., Cho, I.J., Joo, S., Seo, H., Sagong, H.Y., Choi, S.Y., Lee, S.Y., and Kim, K.J. (2019). Rational protein engineering of thermo-stable PETase from *Ideonella sakaiensis* for highly efficient PET degradation. ACS Catal. *9*, 3519–3526.

23. Cui, Y., Chen, Y., Liu, X., Dong, S., Tian, Y.E., Qiao, Y., Mitra, R., Han, J., Li, C., Han, X., et al. (2021). Computational redesign of a PETase for plastic biodegradation under ambient condition by the GRAPE strategy. ACS Catal. *11*, 1340–1350.

24. Lu, H., Diaz, D.J., Czarnecki, N.J., Zhu, C., Kim, W., Shroff, R., Acosta, D.J., Alexander, B.R., Cole, H.O., Zhang, Y., et al. (2022). Machine learning-aided engineering of hydrolases for PET depolymerization. Nature *604*, 662–667.

25. Merrifield, R.B. (1963). Solid phase peptide synthesis. I. Synthesis of a tetrapeptide. J. Am. Chem. Soc. *85*, 2149–2154.

26. Dawson, P.E., Muir, T.W., Clark-Lewis, I., and Kent, S.B.H. (1994). Synthesis of proteins by native chemical ligation. Science *266*, 776–779.

27. Yan, L.Z., and Dawson, P.E. (2001). Synthesis of peptides and proteins without cysteine residues by native chemical ligation combined with desulfurization. J. Am. Chem. Soc. *123*, 526–533.

28. Fang, G.M., Li, Y.M., Shen, F., Huang, Y.C., Li, J.B., Lin, Y., Cui, H.K., and Liu, L. (2011). Protein chemical synthesis by ligation of peptide hydrazides. Angew. Chem. Int. Ed. Engl. *50*, 7645–7649.

29. Milton, R.C., Milton, S.C., and Kent, S.B. (1992). Total chemical synthesis of a D-enzyme: the enantiomers of HIV-1 protease show reciprocal chiral substrate specificity [corrected]. Science *256*, 1445–1448.

30. Vinogradov, A.A., Evans, E.D., and Pentelute, B.L. (2015). Total synthesis and biochemical characterization of mirror image barnase. Chem. Sci. *6*, 2997–3002.

31. Jiang, W., Zhang, B., Fan, C., Wang, M., Wang, J., Deng, Q., Liu, X., Chen, J., Zheng, J., Liu, L., et al. (2017). Mirror-image polymerase chain reaction. Cell Discov. *3*, 17037.

32. Fan, C., Deng, Q., and Zhu, T.F. (2021). Bioorthogonal information storage in L-DNA with a high-fidelity mirror-image *Pfu* DNA polymerase. Nat. Biotechnol. *39*, 1548–1555.

33. Wang, M., Jiang, W., Liu, X., Wang, J., Zhang, B., Fan, C., Liu, L., Pena-Alcantara, G., Ling, J., Chen, J., et al. (2019). Mirror-image gene transcription and reverse transcription. Chem *5*, 848–857.

34. Han, X., Liu, W., Huang, J.W., Ma, J., Zheng, Y., Ko, T.P., Xu, L., Cheng, Y.S., Chen, C.C., and Guo, R.T. (2017). Structural insight into catalytic mechanism of PET hydrolase. Nat. Commun. *8*, 2106.

35. Fecker, T., Galaz-Davison, P., Engelberger, F., Narui, Y., Sotomayor, M., Parra, L.P., Ramírez, C.A., and Sarmiento, C.A. (2018). Active site flexibility as a hallmark for efficient PET degradation by *I. sakaiensis* PETase. Biophys. J. *114*, 1302–1312.

36. Sohma, Y., Sasaki, M., Hayashi, Y., Kimura, T., and Kiso, Y. (2004). Novel and efficient synthesis of difficult sequence-containing peptides through *O-N* intramolecular acyl migration reaction of *O*-acyl isopeptides. Chem. Commun. 124–125.

37. Zeng, W., Li, X., Yang, Y., Min, J., Huang, J.W., Liu, W., Niu, D., Yang, X., Han, X., Zhang, L., et al. (2022). Substrate-binding mode of a thermophilic PET hydrolase and engineering the enzyme to enhance the hydrolytic efficacy. ACS Catal. *12*, 3033–3040.

38. Wan, Q., and Danishefsky, S.J. (2007). Free-radical-based, specific desulfurization of cysteine: a powerful advance in the synthesis of polypeptides and glycopolypeptides. Angew. Chem. Int. Ed. Engl. *46*, 9248–9252.

39. Maity, S.K., Jbara, M., Laps, S., and Brik, A. (2016). Efficient palladium-assisted one-pot deprotection of (acetamidomethyl)cysteine following native chemical ligation and/or desulfurization to expedite chemical protein synthesis. Angew. Chem. Int. Ed. Engl. *55*, 8108–8112.

40. Pastukhov, A.V., and Ropson, I.J. (2003). Fluorescent dyes as probes to study lipid-binding proteins. Proteins *53*, 607–615.

41. Ling, J.J., Fan, C., Qin, H., Wang, M., Chen, J., Wittung-Stafshede, P., and Zhu, T.F. (2020). Mirror-image 5S ribonucleoprotein complexes. Angew. Chem. Int. Ed. Engl. *59*, 3724–3731.

42. Schwabl, P., Köppel, S., Königshofer, P., Bucsics, T., Trauner, M., Reiberger, T., and Liebmann, B. (2019). Detection of various microplastics in human stool: a prospective case series. Ann. Intern. Med. *171*, 453–457.

43. Ragusa, A., Svelato, A., Santacroce, C., Catalano, P., Notarstefano, V., Carnevali, O., Papa, F., Rongioletti, M.C.A., Baiocco, F., Draghi, S., et al. (2021). Plasticenta: first evidence of microplastics in human placenta. Environ. Int. *146*, 106274.

44. Leslie, H.A., Van Velzen, M.J.M., Brandsma, S.H., Vethaak, A.D., Garcia-Vallejo, J.J., and Lamoree, M.H. (2022). Discovery and quantification of plastic particle pollution in human blood. Environ. Int. *163*, 107199.

45. Dintzis, H.M., Symer, D.E., Dintzis, R.Z., Zawadzke, L.E., and Berg, J.M. (1993). A comparison of the immunogenicity of a pair of enantiomeric proteins. Proteins *16*, 306–308.

46. Hartrampf, N., Saebi, A., Poskus, M., Gates, Z.P., Callahan, A.J., Cowfer, A.E., Hanna, S., Antilla, S., Schissel, C.K., Quartararo, A.J., et al. (2020). Synthesis of proteins by automated flow chemistry. Science *368*, 980–987.

47. Gao, R., and Sun, C. (2021). A marine bacterial community capable of degrading poly(ethylene terephthalate) and polyethylene. J. Hazard. Mater. *416*, 125928.

48. Qian, X., Chen, L., Sui, Y., Chen, C., Zhang, W., Zhou, J., Dong, W., Jiang, M., Xin, F., and Ochsenreither, K. (2020). Biotechnological potential and applications of microbial consortia. Biotechnol. Adv. *40*, 107500.

49. Brandon, A.M., Gao, S.H., Tian, R., Ning, D., Yang, S.S., Zhou, J., Wu, W.M., and Criddle, C.S. (2018). Biodegradation of polyethylene

and plastic mixtures in mealworms (larvae of *Tenebrio molitor*) and effects on the gut microbiome. Environ. Sci. Technol. *52*, 6526–6533.

50. Huang, P.S., Boyken, S.E., and Baker, D. (2016). The coming of age of de novo protein design. Nature *537*, 320–327.

51. Mazurenko, S., Prokop, Z., and Damborsky, J. (2020). Machine learning in enzyme engineering. ACS Catal. *10*, 1210–1223.

52. Huang, Y.C., Chen, C.C., Li, S.J., Gao, S., Shi, J., and Li, Y.M. (2014). Facile synthesis of C-terminal peptide hydrazide and thioester of NY-ESO-1 (A39-A68) from an Fmoc-hydrazine 2-chlorotrityl chloride resin. Tetrahedron *70*, 2951–2955.

53. White, P., Keyte, J.W., Bailey, K., and Bloomberg, G. (2004). Expediting the Fmoc solid phase synthesis of long peptides through the application of dimethyloxazolidine dipeptides. J. Pept. Sci. *10*, 18–26.

54. Huang, Y.C., Chen, C.C., Gao, S., Wang, Y.H., Xiao, H., Wang, F., Tian, C.L., and Li, Y.M. (2016). Synthesis of L- and D-ubiquitin by one-pot ligation and metal-free desulfurization. Chemistry *22*, 7623–7628.

55. Brod, F.C., Vernal, J., Bertoldo, J.B., Terenzi, H., and Arisi, A.C. (2010). Cloning, expression, purification, and characterization of a novel esterase from Lactobacillus plantarum. Mol. Biotechnol. *44*, 242–249.